Microstructural evolution and thermal conductivity of diamond/Al composites during thermal cycling

Ping-ping Wang[1),2),*], *Guo-qin Chen*[1),3),*], *Wen-jun Li*[4)], *Hui Li*[1)], *Bo-yu Ju*[1)], *Murid Hussain*[5)], *Wen-shu Yang*[1),3)], *and Gao-hui Wu*[1),3)]

1) School of Materials Science and Engineering, Harbin Institute of Technology, Harbin 150001, China

2) Qiqihar Xiangke New Material Co., Ltd., Qiqihar 161005, China

3) Key Laboratory of Advanced Structure-Function Integrated Materials and Green Manufacturing Technology, School of Material Science and Engineering, Harbin Institute of Technology, Harbin 150001, China

4) Beijing Institute of Spacecraft System Engineering, Beijing 100094, China

5) Department of Chemical Engineering, COMSATS University Islamabad, Lahore Campus, Defence Road, Off Raiwind Road, Lahore 54000, Pakistan

Abstract: The microstructural evolution and performance of diamond/Al composites during thermal cycling has rarely been investigated. In the present work, the thermal stability of diamond/Al composites during thermal cycling for up to 200 cycles was explored. Specifically, the thermal conductivity (λ) of the composites was measured and scanning electron microscopy of specific areas in the same samples was carried out to achieve quasi-*in situ* observations. The interface between the (100) plane of diamond and the Al matrix was well bonded with a zigzag morphology and abundant needle-like Al_4C_3 phases. By contrast, the interface between the (111) plane of diamond and the Al matrix showed weak bonding and debonded during thermal cycling. The debonding length increased rapidly over the first 100 thermal cycles and then increased slowly in the following 100 cycles. The λ of the diamond/Al composites decreased abruptly over the initial 20 cycles, increased afterward, and then decreased monotonously once more with increasing number of thermal cycles. Decreases in the λ of the Al matrix and the corresponding stress concentration at the diamond/Al interface caused by thermal mismatch, rather than interfacial debonding, may be the main factors influencing the decrease in λ of the diamond/Al composites, especially in the initial stages of thermal cycling.

Keywords: metal-matrix composites; diamond; stability; thermal mismatch stress

1. Introduction

Diamond particle-reinforced Al matrix (diamond/Al) composites have been widely investigated on account of their high thermal conductivity (λ) [1] and tailorable coefficient of thermal expansion (CTE) [2], and diamond/Al composites with high performance are urgently needed to be addressed for new generation electronic packaging industry [3]. In-depth research on diamond/Al composites carried out in recent years has mainly focused on the optimization of the preparation method [4–5] and corresponding parameters [6–7] of these composites, microstructural design by process control [8–9], and interfacial engineering [10–11]. Tan *et al.* [12] compared the microstructure and properties of diamond/Al composites fabricated by the vacuum hot pressing and spark plasma sintering methods and concluded that VHPed composites show enhanced λ on account of the good interfacial bonding status of their individual components. Wang *et al.* [13] found that the λ and bending strength of diamond/Al composites prepared by squeeze casting could be improved significantly by 89% (from 321 to 606 W/(m·K)) and 124% (from 98 to 220 MPa), respectively, by controlling their cooling rate. Li *et al.* [14] reported that introduction of a ZrC layer could reduce the amount of Al_4C_3 formed in the resulting composite and demonstrated that a diamond/Al composite bearing the ZrC interface exhibits a high λ of 572 W/(m·K). Ma *et al.* [15] found that addition of a Mo_2C submicron layer coated by a molten-salt route could increase the λ of diamond/Cu composites, while the Mo_2C submicron layer led to the decrease of the λ in diamond/Al composites. Yang *et al.*

*These authors contributed equally to this work.

Corresponding authors: Guo-qin Chen   E-mail: chenguoqin@hit.edu.cn;   Wen-shu Yang   E-mail: yws001003@163.com;

     Gao-hui Wu   E-mail: wugh@hit.edu.cn

[16] and Chen *et al.* [17] found that an interfacial layer of W introduced by magnetron sputtering could enhance the λ (maximum, 622 W/(m·K)) and bending (maximum, 304 MPa) properties of diamond/Al composites. Overall, these studies support efforts to significantly enhance the λ of diamond/Al composites.

While extensive research on the design of the interfacial microstructure and corresponding λ of diamond/Al composites has been carried out, by contrast, the microstructural evolution and performance of diamond/Al composites under simulated service conditions have been rarely reported. Diamond/Al composites could be mainly applied in thermal management systems because of their ability to endure high heat–moisture environments and thermal cycling. Thus, understanding the stability and evolution of the properties of these composites is essential to expand their applications. Limited research on the stability of composites in a high heat–moisture environment has been carried out. Monje *et al.* [18] reported that diamond/Al composites with small amounts of Al_4C_3 are highly prone to remarkable decreases in λ, which contradicts the findings of Yang *et al.* [19], who showed that the λ of similar composites decreases by only 17% because of the decomposition of Al_4C_3. Yang *et al.* [19] and Xin *et al.* [20] reported that the thermal stability of diamond/Al composites could be greatly improved by the interfacial layer design of W and WC. Thus far, only Monje *et al.* [18] have reported that diamond/Al composites with small amounts of Al_4C_3 show poor stability on account of their interfacial debonding characteristics. Indeed, the in-depth microstructural evolution and variation of properties of diamond/Al composites have yet to be fully understood.

In the present work, the thermal stability of diamond/Al composites during thermal cycling from −65 to 150°C for up to 200 cycles was explored. The evolution of the interfacial bonding of the composites was also investigated, and the variation of λ as a function of number of thermal cycles was assessed.

2. Experimental

Diamond particles with mean size of 100 μm (MBD4; Henan Famous Diamond Industries) and commercial-grade Al (1060, 99.6wt% purity; Northeast Light Alloy Co., Ltd., China) were used as raw materials in the present study. Diamond/Al composites (58vol%) were synthesized via an optimized squeeze-casting method as reported in detail in our previous work [13]. The as-received diamond powder was tap-packed into a graphite mold assembled in a steel cylinder and then preheated at 800°C. The tap-packed diamond powder was then infiltrated with pressurized liquid Al that had been preheated to 850°C. Sufficient solidification was achieved after approximately 20 min of melt pressurization. Six samples measuring ϕ12.7 mm × 3 mm in size were pre-

pared and then thermal-cycled; specifically, five samples were used for the λ test and one sample was used for microstructural observations. The thermal cycling treatments were performed in a thermal shock chamber with a temperature accuracy of 5°C (Jinan Shidai Mountain Instrument Co., Ltd., China) according to GJB548B-2005. The thermal cycling treatments were carried out from −65 to 150°C for up to 200 cycles with a shift time from −65 to 150°C less than 1 min. Each shift was maintained at the set temperature for 10 min, as shown in Fig. 1.
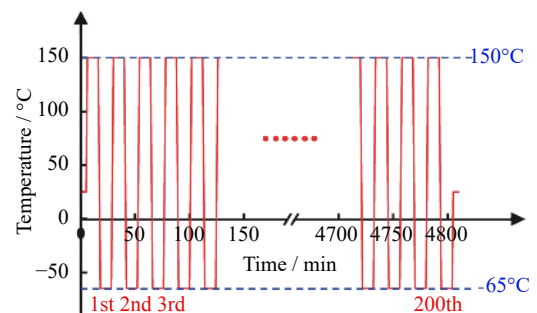

Fig. 1.   Schematic process of the thermal cycling treatment employed in the present work.

The morphology of the polished surfaces of the diamond/Al composites was observed by scanning electron microscopy (SEM; FEI Quanta 200FEG) during thermal cycling. Areas of interest in the composites were marked out for further observation of their microstructural evolution after a predetermined number of thermal cycles. Thus, quasi-*in situ* observations were achieved. The composite samples were polished by a cross-section polishing machine (IB-09020CP, JEOL) working at an acceleration voltage of 6 kV and gun currents of 150–180 μA.

Transmission electron microscopic (TEM) observations were conducted on a JEL-2100 transmission electron microscope (JEOL Ltd.) working at an acceleration voltage of 200 kV, while the TEM samples were prepared on a FEI Helios NanoLab 600i focused ion beam scanning electron microscope (FIB SEM) equipped with a micromanipulator (Omniprobe Autoprobe 200.2 micromanipulator, Dallas, TX). The thermal diffusivity (k) of the samples was measured by an LFA 447 Nanoflash instrument (NETZSCH GmbH, Selb, Germany) at room temperature. The λ of the composites was calculated by using the following equation: $\lambda = k \times \rho \times C_p$, where ρ and C_p are the density and specific heat, respectively, of the diamond/Al composites, ρ could be determined by the Archimedes method, and C_p could be calculated according to the law of mixtures. Five samples of each composite were measured to ensure the statistical significance of the results. Moreover, the λ tests were carried out using the same five samples throughout 200 thermal cycles to eliminate errors that may be introduced by other factors.

3. Results and discussion

3.1. Microstructure of the diamond/Al composites

3.1.1. Microstructure of the diamond/Al composites before thermal cycling

Representative microstructures of the diamond particles are shown in Fig. 2. As widely reported in the literature, the diamond particles show an octahedral morphology with rectangular (100) and hexagonal (111) surface planes [21]; high-magnification images of these planes are shown in Figs. 2(a)–2(d), respectively. Several growth steps, which are likely due to the rapid growth of diamond particles [22], are observed on the surfaces of the particles, and even more steps are observed in the (100) plane. Compared with the (100) plane (Figs. 2(a) and 2(b)), the (111) surface plane of the diamond particles is clearly flatter (Figs. 2(c) and 2(d)). Che *et al.* [23] measured the roughness of the (100) and (111) planes of diamond particles by atomic force microscopy and reported that both surfaces are rather smooth with height variations of only several nanometers.
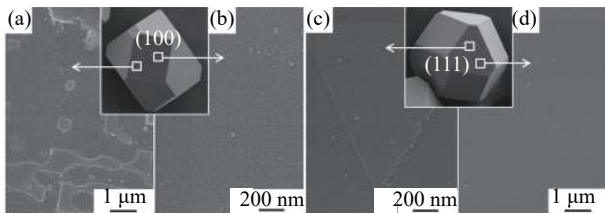

Fig. 2. **Representative microstructures and high-magnification images of the (a, b) (100) and (c, d) (111) surface planes of the diamond particles.**

The SEM microstructure of the polished surface of the prepared diamond/Al composites obtained before thermal cycling is shown in Fig. 3. The dark black and continuous phases reflect diamond and the Al matrix, respectively. Bright gray phases measuring several hundred of nanometers in size (yellow arrows) reflect the interface between diamond and Al. Interestingly, the distribution of these gray phases occurs only on certain diamond surfaces; other surfaces marking interfaces between diamond and the Al matrix are relatively clean.
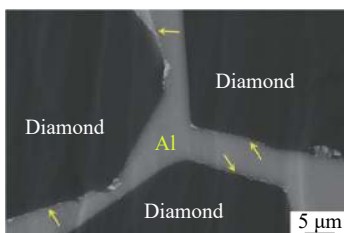

Fig. 3. **SEM microstructure of the polished surface of the prepared diamond/Al composites.**

TEM micrographs of a clean interface and an interface with bright gray phases are shown in Fig. 4. The corresponding selected area diffraction patterns in Figs. 4(b) and 4(e) respectively reveal the (111) and (100) planes of the diamond particles. The bright gray phases observed at the interface between the (100) plane of diamond and the Al matrix are needle-like Al_4C_3 (Fig. 4(f)). Because the surface energy of the (111) plane is much lower than that of the (100) plane [24], selective interfacial bonding behavior has been widely reported in diamond-reinforced metal-matrix composites [25–27]. The interface between the (111) plane of diamond and the Al matrix is rather flat. In our previous work, the measured height variation of the (111) surface of diamond particles is ~4.7 nm [16], which is close to the height variation of annealed diamond reported by Che *et al.* [23]. Because no interfacial product is formed between the (111) plane of diamond and the Al matrix, the bonding mode of this interface could be mainly attributed to mechanical bonding, which is rather weak on account of the very smooth surface of diamond. Besides needle-like Al_4C_3, several steps are observed on the (100) plane of diamond. Therefore, the bonding mode between the (100) plane of diamond and the Al matrix is a combination of chemical and mechanical bonding. The bonding strength of this interface may be expected to be fairly high because of its zigzag morphology.
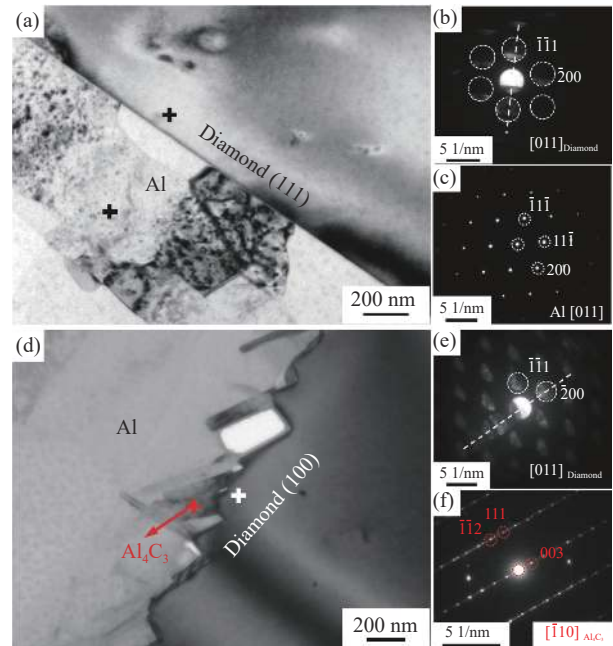

Fig. 4. **TEM observation of the interface between diamond particles and the Al matrix. (a) Interface between the (111) plane of diamond and Al. (b, c) Selected area diffraction (SAED) patterns of (b) diamond and (c) Al in (a). (d) Interface between the (100) plane of diamond Al. (e, f) SAED patterns of (e) diamond and (f) Al_4C_3 in (d).**

3.1.2. Microstructural evolution of the diamond/Al interface during thermal cycling

Representative microstructures of the same areas in the

diamond/Al composites before and after thermal cycling (200 cycles) are shown in Figs. 5(a) and 5(b), respectively. No significant change is observed in the interface between the (100) plane of diamond and the Al matrix with needle-like Al_4C_3 (yellow dashed box, Fig. 5(a)) over the course of thermal cycling. By contrast, significant debonding occurs in the interface between the (111) plane of diamond and the Al matrix (red dashed box, Fig. 5(b)); this debonding may be due to

the weak bonding characteristics of the interface. Because the CTEs of Al and diamond particles are remarkably difference, thermal cycling may generate high levels of thermal mismatch stress, which causes the visco-plastic deformation of the Al matrix. The variation in volume (ΔV_m) between a solid matrix v_m and a rigid particle arrangement of metal-matrix composites can be estimated in terms of the volume fraction of the matrix by using Eq. (1) [28]:
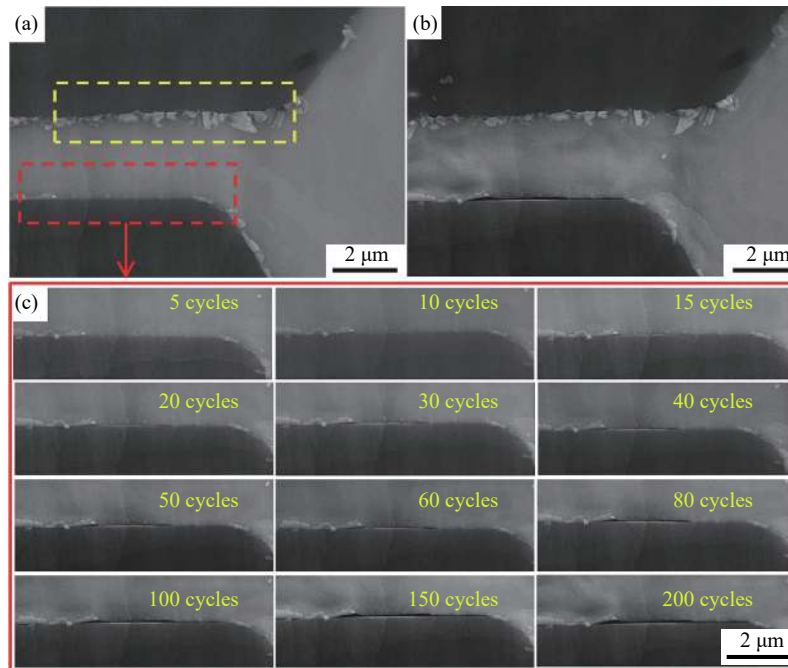

Fig. 5. Representative microstructure of the same area of a diamond/Al composite (a) before and (b) after 200 thermal cycles (no interfacial debonding was occurred in the area marked by the yellow dashed box). (c) Changes in the microstructure of the area marked by the red dashed box in (a) as the number of thermal cycles increases from 5 to 200.

$$\Delta V_m = 3v_m(CTE_m - CTE_p)\Delta T \qquad (1)$$

where the subscripts m and p refer to the matrix and particles, respectively, and ΔT is the temperature difference during thermal cycling.

Because the volume content of the Al matrix in the composite is approximately 42%, the CTE of Al is ~23×10^{-6}/°C, the CTE of diamond is 2.3×10^{-6}/°C, and ΔT is 215°C, the calculated volume variation is approximately 0.56%. Only a small fraction of deformation (<0.1%) could be accommodated by elastic strain [28]. Therefore, extensive residual visco-plastic deformation may occur in the composite and lead to permanent interfacial debonding between the (111) plane of the diamond particles and the Al matrix. By comparison, enhanced interfacial bonding between the (100) plane of the diamond particles and Al matrix due to mechanical occlusion and the presence of needle-like Al_4C_3 with a moderate CTE (~8×10^{-6}/°C) could compensate for the thermal stress that develops at the diamond/Al interface over the course of thermal cycling. Therefore, no interfacial debonding is observed between the (100) plane of the diamond

particles and the Al matrix.

Changes in the microstructure of the area marked by the red dashed box in Fig. 5(a) were observed as the number of thermal cycles increased from 5 to 200, as shown in Fig. 5(c), to assess the interfacial debonding process of this area. Very weak debonding is observed within the first 10 thermal cycles. However, as the number of cycles increases, interfacial debonding becomes more significant and the debonding length gradually increases. Changes in debonding length measured from Fig. 5(c) are shown in Fig. 6. The debonding length increases quickly in a nearly linear manner from 0 to 6.2 μm in the first 100 cycles and then increases very slow to 6.7 μm in the following 100 cycles. The variation of the debonding length (L) of the diamond/Al composite with the cycle number (n) could be fitted using Eq. (2) with an adjusted R^2 value of 0.97754. Eq. (2) reveals that the debonding length could be expected to grow very slowly with further increases in thermal cycling, thus implying that thermal mismatch stress could be well relaxed by debonding of the diamond/Al interface.
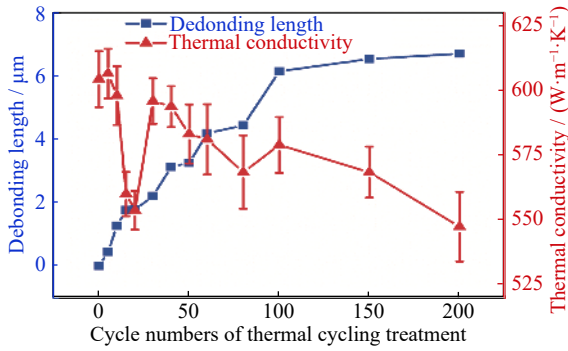
Fig. 6. Variation of the debonding length measured from Fig. 5 and thermal conductivity of the diamond/Al composite during thermal cycling.

$$L = 7.48788 - 7.37929 \times 0.98711^{n} \qquad (2)$$

3.2. Evolution of the thermal conductivity of the diamond/Al composites

The variation of the λ of the diamond/Al composites during thermal cycling is shown in Fig. 6. In general, λ decreases with increasing cycle number, which agrees well with the results reported by Monje *et al.* [18] and Bai *et al.* [29]. Monje *et al.* [18] measured the λ of diamond/Al composites after 100–1000 cycles and observed a monotonous decrease in this property. However, in the present work, the λ of the diamond/Al composite initially decreases abruptly in the first 20 cycles to a minimum value, increases to a relatively high value, and then decreases monotonously once more with increasing number of thermal cycles. The λ of the diamond/Al composite observed after 20 cycles (553 W/(m·K)) is close to that obtained after 200 cycles (547 W/(m·K)). The λ of the Al matrix composite reinforced with 40 μm diamond particles (named as 40 μm-diamond/Al composite) was measured during thermal cycling to confirm this unusual result, as shown in Fig. 7. The λ of the 40 μm-diamond/Al composite clearly showed a trend similar to that of the 100 μm-diamond/Al composite (Fig. 6).

3.3. Mechanism of the evolution of the thermal conductivity of diamond/Al composites during thermal cycling

The λ of particle-reinforced metal-matrix composites could be well described by the Hasselman and Johnson (H–J) model, which is expressed as [30]:

$$\lambda_{c} = \lambda_{Al} \cdot \frac{2V_{Dia}(\frac{\lambda_{Dia}}{\lambda_{Al}} - \frac{\lambda_{Al}}{ah_{c}} - 1) + \frac{\lambda_{Dia}}{\lambda_{Al}} + 2\frac{\lambda_{Dia}}{ah_{c}} + 2}{V_{Dia}(1 - \frac{\lambda_{Dia}}{\lambda_{Al}} + \frac{\lambda_{Dia}}{ah_{c}}) + \frac{\lambda_{Dia}}{\lambda_{Al}} + 2\frac{\lambda_{Dia}}{ah_{c}} + 2} \qquad (3)$$

where λ and V respectively refer to thermal conductivity and volume; the subscripts c, Dia, and Al respectively refer to the composite, diamond particles, and Al matrix; a is the average radius of the particles; and h_{c} is the interfacial thermal conductance of the composites.
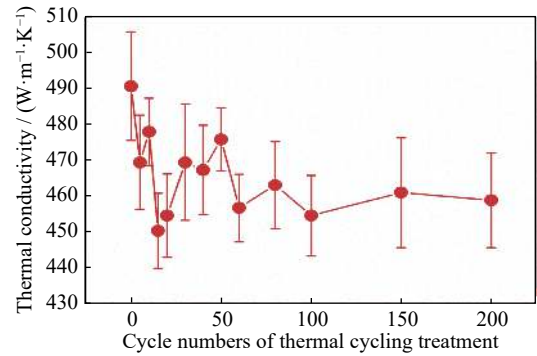

Fig. 7. Variation of the thermal conductivity of the 40 μm-diamond/Al composite during thermal cycling.

If the λ of the Al matrix and diamond particles and their corresponding volume contents are considered constant during thermal cycling, the h_{c} of the composites decreases from approximately 3.2×10^{8} to 1.9×10^{8} W/(m²·K) during the first 20 thermal cycles, increases to approximately 2.9×10^{8} W/(m²·K), and then decreases once more to approximately 1.8×10^{8} W/(m²·K). The corrected interfacial thermal conductance (h^{*}) could be calculated simplistically as follows:

$$h^{*} = \frac{L_{0} - L_{c}}{L_{0}} h_{c} \qquad (4)$$

where L_{0} is the average side length of the diamond particle surface (~55 μm) and L_{c} is the length of the debonded interface.

If only interfacial debonding is considered (i.e., 6.7 μm after 200 cycles) and the average length of the (111) plane of the diamond particles is set to 55 μm, the h_{c} of the composites only decreases from $\sim3.2 \times 10^{8}$ to 2.8×10^{8} W/(m²·K), as shown in Fig. 8, which is far higher than the calculated value of 1.8×10^{8} W/(m²·K). Therefore, interfacial debonding may not be the sole factor responsible for the observed decrease in λ, and some other factor may contribute more significantly to the λ of the diamond/Al composites. In general, the λ of the diamond/Al composites is affected by the properties of the Al matrix, the diamond reinforcement, and the interfacial bonding status of the composite. Because the content and λ of the diamond particles may be considered constant, only the λ of the Al matrix may vary in this system. If the effect of interfacial debonding and thermal stress concentration at the interface is neglected and the h_{c} of the composite is fixed to 3.2×10^{8} W/(m²·K), the λ of the Al matrix decreases from 237 to 199 W/(m·K) and the λ of the composites decreases from 606 W/(m·K) to 547 W/(m·K). The effect of interfacial debonding may further decrease the λ of the Al matrix to 205 W/(m·K). Generation of a high density of crystal defects has been reported to occur during thermal cycling because of the high thermal mismatch stress generated in the system [31–32], which could remarkably decrease the λ of the Al matrix [33]. Thus, rather than interfacial debonding, which

has been widely cited to explain decreases in λ in diamond/Al composites, the decrease in λ of the Al matrix caused by thermal mismatch stress accumulation could be considered the main factor influencing the change in the λ of these composites.
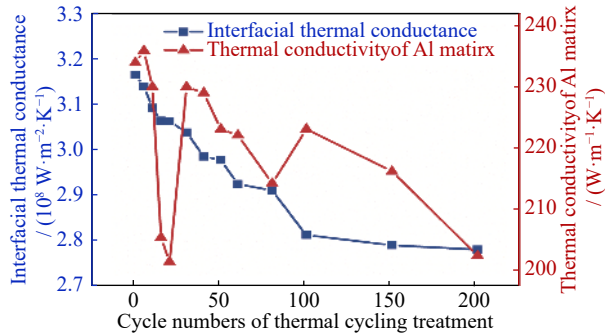

Fig. 8. Variation of the derived interfacial thermal conductance and thermal conductivity of the Al matrix during thermal cycling.

The effect of thermal stress concentration at the interface of the diamond/Al matrix on the h_c of the composite shows a linear trend. However, the effect of interfacial thermal stress on the interfacial thermal conductance and thermal conductivity of the Al matrix reveals a nonlinear trend, which may affect the λ of the composites. Thus, besides interfacial debonding, which leads to a decrease in the λ of the diamond/Al composites, nonlinear decreases in the λ of the Al matrix and the effect of interfacial thermal stress on interfacial thermal conductance may explain the observed decrease in λ in the initial 20 thermal cycles. The actual contributions of these factors should be established in future investigations.

Chemical decomposition [34] and the presence of Al_4C_3 could increase the vulnerability of diamond/Al composites to moist environments [20], which limits their applications. Therefore, a transition interface with a moderate CTE that could match dimensional changes during thermal cycling and good strength/toughness to relax the generated thermal mismatch stress may be an important approach to improve the λ of diamond/Al composites during thermal cycling.

4. Conclusions

In the present work, changes in the thermal stability and interfacial microstructural evolution of diamond/Al composites during thermal cycling from −65 to 150ºC for up to 200 cycles were explored.

(1) The (100) plane of diamond shows a zigzag morphology, and several needle-like Al_4C_3 phases are observed at the interface between this plane and the Al matrix. The absence of a significant change in the interface of the (100) plane of diamond and the Al matrix after 200 thermal cycles is attributed to enhanced interfacial bonding between these phases.

However, the interface between the (111) plane of diamond and the Al matrix is very flat, and no interfacial product is observed. This interface reveals debonding after 200 thermal cycles because of stress accumulation due to thermal mismatch. Further observation indicates that the debonding length of this interface initially increases rapidly within the first 100 cycles from 0 to 6.2 μm and then increases very slow to 6.7 μm in the following 100 cycles, thereby implying that thermal mismatch stress could be well relaxed by debonding.

(2) The λ of the diamond/Al composites initially decreases abruptly from 604 to 553 W/(m·K) in the first 20 thermal cycles, increases to 595 W/(m·K) afterward, and then decreases monotonously once more with increasing number of thermal cycles. Changes in the λ of the diamond/Al composites are discussed on the basis of the H–J model. Results suggest that, rather than interfacial debonding, which is widely cited to explain decreases in λ in diamond/Al composites, decreases in the λ of the Al matrix arising from stress accumulation due to thermal mismatch appears to be the main factor influencing the λ of these composites, especially in the initial period of cycling.

Acknowledgements

References

[1] Z.F. Che, J.W. Li, Q.X. Wang, L.H. Wang, H.L. Zhang, Y. Zhang, X.T. Wang, J.G. Wang, and M.J. Kim, The formation of atomic-level interfacial layer and its effect on thermal conductivity of W-coated diamond particles reinforced Al matrix composites, *Compos. A: Appl. Sci. Manuf.*, 107(2018), p. 164.

[2] J.P. Long, X. Li, D.D. Fang, P. Peng, and Q. He, Fabrication of diamond particles reinforced Al-matrix composites by hot-press sintering, *Int. J. Refract. Met. Hard Mater.*, 41(2013), p. 85.

[3] I.E. Monje, E. Louis, and J.M. Molina, Interfacial nano-engineering in Al/diamond composites for thermal management by *in situ* diamond surface gas desorption, *Scr. Mater.*, 115(2016), p. 159.

[4] O. Beffort, F.A. Khalid, L. Weber, P. Ruch, U.E. Klotz, S. Meier, and S. Kleiner, Interface formation in infiltrated Al(Si)/diamond composites, *Diam. Relat. Mater.*, 15(2006), No. 9, p. 1250.

[5] C.X. Li, X.T. Wang, L.H. Wang, J.W. Li, H.X. Li, and H.L. Zhang, Interfacial characteristic and thermal conductivity of Al/diamond composites produced by gas pressure infiltration in a nitrogen atmosphere, *Mater. Des.*, 92(2016), p. 643.

[6] Y. Zhang, J.W. Li, L.L. Zhao, and X.T. Wang, Optimisation of high thermal conductivity Al/diamond composites produced by gas pressure infiltration by controlling infiltration temperature and pressure, *J. Mater. Sci.*, 50(2015), No. 2, p. 688.

[7] K. Chu, C.C. Jia, X.B. Liang, and H. Chen, Effect of sintering temperature on the microstructure and thermal conductivity of Al/diamond composites prepared by spark plasma sintering, *Int. J. Miner. Metall. Mater.*, 17(2010), No. 2, p. 234.

[8] J. Shi, R.C. Che, C.Y. Liang, Y. Cui, S.B. Xu, and L. Zhang, Microstructure of diamond/aluminum composites fabricated by pressureless metal infiltration, *Compos. B: Eng.*, 42(2011), No. 6, p. 1346.

[9] I.E. Monje, E. Louis, and J.M. Molina, Aluminum/diamond composites: A preparative method to characterize reactivity and selectivity at the interface, *Scr. Mater.*, 66(2012), No. 10, p. 798.

[10] Z.Q. Tan, Z.Q. Li, G.L. Fan, Q. Guo, X.Z. Kai, G. Ji, L.T. Zhang, and D. Zhang, Enhanced thermal conductivity in diamond/aluminum composites with a tungsten interface nanolayer, *Mater. Des.*, 47(2013), p. 160.

[11] G. Ji, Z.Q. Tan, Y.G. Lu, D. Schryvers, Z.Q. Li, and D Zhang, Heterogeneous interfacial chemical nature and bonds in a W-coated diamond/Al composite, *Mater. Charact.*, 112(2016), p. 129.

[12] Z.Q. Tan, G. Ji, A. Addad, Z.Q. Li, J.F. Silvain, and D. Zhang, Tailoring interfacial bonding states of highly thermal performance diamond/Al composites: Spark plasma sintering vs. vacuum hot pressing, *Compos. A: Appl. Sci. Manuf.*, 91(2016), p. 9.

[13] P.P. Wang, Z.Y. Xiu, L.T. Jiang, G.Q. Chen, X. Lin, and G.H. Wu, Enhanced thermal conductivity and flexural properties in squeeze casted diamond/aluminum composites by processing control, *Mater. Des.*, 88(2015), p. 1347.

[14] N. Li, L.H. Wang, J.J. Dai, X.T. Wang, J.G. Wang, M.J. Kim, and H.L. Zhang, Interfacial products and thermal conductivity of diamond/Al composites reinforced with ZrC-coated diamond particles, *Diamond Relat. Mater.*, 100(2019), art. No. 107565.

[15] S.D. Ma, N.Q. Zhao, C.S. Shi, E.Z. Liu, C.N. He, F. He, and L.Y. Ma, Mo_2C coating on diamond: Different effects on thermal conductivity of diamond/Al and diamond/Cu composites, *Appl. Surf. Sci.*, 402(2017), p. 372.

[16] W.S. Yang, G.Q. Chen, P.P. Wang, J. Qiao, F.J. Hu, S.F. Liu, Q. Zhang, M. Hussain, R.H. Dong, and G.H. Wu, Enhanced thermal conductivity in Diamond/Aluminum composites with tungsten coatings on diamond particles prepared by magnetron sputtering method, *J. Alloys Compd.*, 726(2017), p. 623.

[17] G.Q. Chen, W.S. Yang, L. Xin, P.P. Wang, S.F. Liu, J. Qiao, F.J. Hu, Q. Zhang, and G.H. Wu, Mechanical properties of Al matrix composite reinforced with diamond particles with W coatings prepared by the magnetron sputtering method, *J. Alloys Compd.*, 735(2018), p. 777.

[18] I.E. Monje, E. Louis, and J.M. Molina, Role of Al_4C_3 on the stability of the thermal conductivity of Al/diamond composites subjected to constant or oscillating temperature in a humid environment, *J. Mater. Sci.*, 51(2016), No. 17, p. 8027.

[19] W.L. Yang, K. Peng, J.J. Zhu, D.Y. Li, and L.P. Zhou, Enhanced thermal conductivity and stability of diamond/aluminum composite by introduction of carbide interface layer, *Diamond Relat. Mater.*, 46(2014), p. 35.

[20] L. Xin, X. Tian, W.S. Yang, G.Q. Chen, J. Qiao, F.J. Hu, Q. Zhang, and G.H. Wu, Enhanced stability of the Diamond/Al composites by W coatings prepared by the magnetron sputtering method, *J. Alloys Compd.*, 763(2018), p. 305.

[21] M. Battabyal, O. Beffort, S. Kleiner, S. Vaucher, and L. Rohr, Heat transport across the metal–diamond interface, *Diamond Relat. Mater.*, 17(2008), No. 7-10, p. 1438.

[22] L.T. Jiang, P.P. Wang, Z.Y. Xiu, G.Q. Chen, X. Lin, C. Dai, and G.H. Wu, Interfacial characteristics of diamond/aluminum composites with high thermal conductivity fabricated by squeeze-casting method, *Mater. Charact.*, 106(2015), p. 346.

[23] Z.F. Che, Y. Zhang, J.W. Li, H.L. Zhang, X.T. Wang, C. Sun, J.G. Wang, and M.J. Kim, Nucleation and growth mechanisms of interfacial Al_4C_3 in Al/diamond composites, *J. Alloys Compd.*, 657(2016), p. 81.

[24] T. Halicioglu, Calculation of surface energies for low index planes of diamond, *Surf. Sci.*, 259(1991), No. 1-2, p. L714.

[25] G. Chang, F.Y. Sun, J.L. Duan, Z.F. Che, X.T. Wang, J.G. Wang, M.J. Kim, and H.L. Zhang, Effect of Ti interlayer on interfacial thermal conductance between Cu and diamond, *Acta Mater.*, 160(2018), p. 235.

[26] Z.Q. Tan, Z.Q. Li, G.L. Fan, X.Z. Kai, G. Ji, L.T. Zhang, and D. Zhang, Diamond/aluminum composites processed by vacuum hot pressing: Microstructure characteristics and thermal properties, *Diamond Relat. Mater.*, 31(2013), p. 1.

[27] G. Chang, F. Y. Sun, L.H. Wang, Z.X. Che, X.T. Wang, J.G. Wang, M.J. Kim, and H.L. Zhang, Regulated interfacial thermal conductance between Cu and diamond by a TiC interlayer for thermal management applications, *ACS Appl. Mater. Interfaces*, 11(2019), No. 29, p. 26507.

[28] M. Schöbel, H.P. Degischer, S. Vaucher, M. Hofmann, and P. Cloetens, Reinforcement architectures and thermal fatigue in diamond particle-reinforced aluminum, *Acta Mater.*, 58(2010), No. 19, p. 6421.

[29] G.Z. Bai, Y.J. Zhang, X.Y. Liu, J.J. Dai, X.T. Wang, and H.L. Zhang, High-temperature thermal conductivity and thermal cycling behavior of Cu–B/diamond composites, *IEEE Trans. Compon. Packag. Manuf. Technol.*, 10(2020), No. 4, p. 626.

[30] D.P.H. Hasselman and L.F. Johnson, Effective thermal conductivity of composites with interfacial thermal barrier resistance, *J. Compos. Mater.*, 21(1987), No. 6, p. 508.

[31] P. Kot, A. Baczmański, E. Gadalińska, S. Wroński, M. Wróński, M. Wróbel, G. Bokuchava, C. Scheffzük, and K. Wierzbanowski, Evolution of phase stresses in Al/SiC_p composite during thermal cycling and compression test studied using diffraction and self-consistent models, *J. Mater. Sci. Technol.*, 36(2020), p. 176.

[32] J.P. Liu, D.B. Xiong, Y.S. Su, Q. Guo, Z.Q. Li, and D. Zhang, Effect of thermal cycling on the mechanical properties of carbon nanotubes reinforced copper matrix nanolaminated composites, *Mater. Sci. Eng. A*, 739(2019), p. 132.

[33] R. Zare, H. Sharifi, M.R. Saeri, and M. Tayebi, Investigating the effect of SiC particles on the physical and thermal properties of $Al6061/SiC_p$ composite, *J. Alloys Compd.*, 801(2019), p. 520.

[34] B.Y. Ju, W.S. Yang, P.Z. Shao, M. Hussain, Q. Zhang, Z.Y. Xiu, X.W. Hou, J. Qiao, and G.H. Wu, Effect of interfacial microstructure on the mechanical properties of GNPs/Al composites, *Carbon*, 162(2020), p. 346.